

Streamlining CubeSat Solar Panel Fabrication Processes

Ariel Sandberg
 University of Michigan, Michigan Exploration Laboratory
 11589 E Lake Avenue, Englewood, CO 80111
 arimberg@umich.edu

Faculty Advisor: Dr. Timothy Smith
 University of Michigan, Aerospace Engineering

ABSTRACT

A critical facet of CubeSat fabrication is solar panel characterization and assembly. Though capable of producing flight quality solar subsystems, traditional methods of solar panel fabrication contain intrinsic inefficiencies and inconsistencies that compromise the subsystem's overall reliability. Taking Michigan Exploration Laboratory's (MXL) heritage solar panel procedures as a case study, this investigation sought to streamline the solar panel fabrication process to increase its yield, cost effectiveness and consistent production. Four main aspects of solar panel fabrication were targeted for improvement, specifically: solar cell tabbing, solar cell stringing, solar cell adhesion to the substrate and cell coverglass integration. Through synthesizing best practices and procedures, a robust process was developed that greatly increases panel manufacturability and performance. This procedure was verified via various methods including vibration testing and thermal-vacuum testing and will be implemented on MXL's upcoming TBEx CubeSat mission.

INTRODUCTION

For manufacturers like MXL that fabricate their solar panels in-house, the solar panel procedure can be commonly distilled into four main steps: cell tabbing, cell stringing, cell adhesion to the printed circuit board and coverglass application. The following is a discussion of the heritage methods for these procedural steps, as exemplified by MXL, and their intrinsic problems.

To be electrically viable, solar cells must be "tabbed" with interconnects that connect the cells to the electrical power circuit. Today, space-grade solar cells can be purchased with these tabs pre-integrated (known as "CIC'd" cells), or bare, requiring in-house integration.⁽³⁾ Bare cells,

such as the BTJM cells employed by MXL, are often selected over CIC'd cells for their lower costs and shorter lead times.

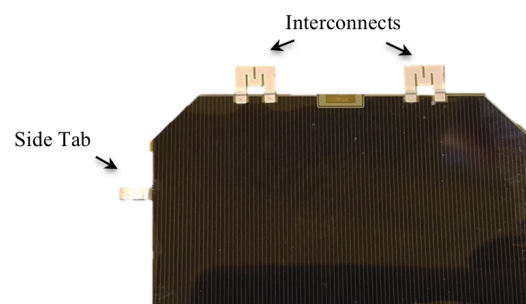


Figure 1: EMCORE Multi-Junction BTJM cells used by MXL, with tabs.

Historically, MXL's procedure for applying tabs to cells was relatively complex, requiring numerous instruments (a hot

plate, a soldering iron and a reflow gun), three heating cycles and the use of weights on cell faces to increase the strength of solder joints. The complexity of this tabbing procedure not only consumed undue labor (2 fabricators) and time (~10 minutes per cell); it also posed a risk of cell shorting. Due to the frequent heating and reheating of the cells, unintentional solder flow regularly caused shorts by connecting the cell's negative pads to its positive backside, eliminating the cell's power production capabilities. Furthermore, the use of elements such as weights posed a physical risk to the fragile cells.

Once tabbed, cells are assembled into panels, the first step of which often involves "stringing" them in series. Traditional methods of cell stringing commonly involve directly soldering cells to one another via tabs. In the case of MXL's CADRE satellite, cells were strung together via interconnects that connected a cell's negative terminals to the positive backside of its adjacent cell (see Figure 2).



Figure 2: MXL's heritage method of solar cell stringing.

Such direct stringing was justified on the basis of maximizing the number of cells that could be integrated onto a given printed circuit board (PCB); however, in practice, this procedure was observed to compromise solar string manufacturability, reparability and versatility.

During CADRE flight build, strings of up to six cells were fabricated through direct soldering, involving extensive cell handling and significant challenges to cell repair and placement. As present in the tabbing procedure, weights were used to strengthen the solder joints while stringing. If a cell was damaged during the heating process, a multi-step procedure utilizing a reflow gun was needed to reflow the solder paste on the tabs. The extra heating cycles and handling required to then integrate an additional cell into the string often resulted in damage to other cells. Furthermore, direct stringing restricted cells to a vertical orientation, limiting the flexibility with which cells could be placed on the solar PCB (creative orientation of solar cells is often necessary to accommodate unique structural elements of a given bus).

After stringing, cells require adhering to the PCB substrate. A common heritage method of cell adherence is via epoxy, or in MXL's case, a silicon adhesive applied via putty knife (see Figure 3). As exemplified by MXL, this traditional procedure contained numerous problems. First, the silicon adhesive demonstrated a high incidence of voiding (air pockets trapped beneath the cell) due to the difficulties of uniformly applying the adhesive to the PCB cell pad. When voids are exposed to the vacuum of space, escaping air can cause severe damage to solar cells, compromising the satellite's power generation. Thus, a panel that exhibits voiding is unviable for flight. Because voiding could not be corrected once the silicon adhesive cured, it rendered entire panels unusable, resulting in wasted time and lab resources.

In addition to the voiding risk, this process was time intensive, requiring 30-45 minutes for application and a four-hour curing time. This preparation and curing time made manufacturing solar panels on a quick timescale difficult. The space-grade silicon

adhesive itself was expensive, costing the lab hundreds of dollars per flight build. Furthermore, the properties of the cured silicon adhesive made it extremely difficult to remove problematic cells from integrated strings, often making it more time effective to fabricate entirely new panels than to try to salvage ones with damage.



Figure 3: Applying silicon epoxy to PCB with putty knife.

Though coverglass is not strictly necessary for satellites with brief scientific missions, it is widely viewed as desirable because it physically protects the fragile cells while limiting their on-orbit degradation.

According to a study conducted by the Department of Earth and Space Sciences at UCLA ⁽⁷⁾, cells without coverglass will significantly degrade while in-orbit; specifically, cells can lose up to 30% of power production capabilities after only two years due to factors like UV radiation, atomic oxygen degradation and high-energy particle radiation. However, with coverglass, the observed degradation can be reduced to around 10% for a two year mission. Solar panel fabricators that purchase bare cells are tasked with applying coverglass to their cells in-house.

PROCESS IMPROVEMENTS

Overview

The following procedural changes were implemented to streamline the solar panel fabrication process:

Tabbing: The tabbing procedure was significantly improved. In lieu of multiple heating elements, a single heating element was used (a reflow gun) to solder the top interconnects and side tab. Furthermore, the need for dangerous elements such as weights on cell faces was eliminated. This procedure was developed in collaboration with Andrew Dahir of CU-Boulder's QB50 team. ⁽²⁾

Stringing: The previous method of directly stringing cells was replaced by stringing the cells via the PCB substrate. A PCB was designed that allows the cells to be decoupled and soldered directly to the PCB substrate. Several other CubeSat teams have experimented with such decoupling to great success, including CalPoly's CP1 team ⁽⁶⁾ and CU's QB50 team.

Adhering: A procedure was developed that replaces the previously utilized silicon adhesive to adhere the cells to the panel with double-sided Kapton tape. Double-sided Kapton tape with pressure sensitive adhesive is an emerging method with variations on flight systems constructed by The Aerospace Corporation ⁽⁴⁾ and the Laboratory for Atmospheric and Space Physics in Boulder, CO ⁽⁵⁾. To supplement easy alignment of cells on the PCB, an alignment jig was created that can be easily modified and reprinted via 3D printer for future PCB iterations.

Coverglass: A robust, simple coverglass procedure was developed that protects the cells with negligible loss to power. Nusil EPM-2420 Low Volatility General Purpose

Silicone Adhesive was selected as the top candidate for coverglass adhesion. This adhesive was selected for its low viscosity, low volatility, affordability and easily reproducible curing conditions.

While these procedural changes were implemented in the context of MXL, they can be readily translated to other solar panel fabrication settings.

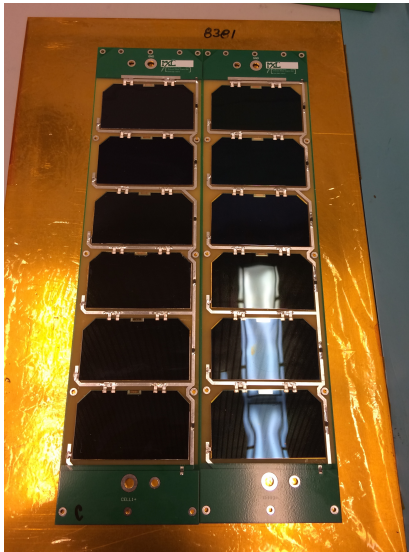


Figure 4: Two completed solar panels utilizing the streamlined fabrication processes.

Verification Methods

The following verification methods were used to assess the procedural improvements.

Electroluminescence (EL) Testing: Each cell was subjected to EL testing throughout the integration process (post-tabling, post-stringing and post-integration onto PCB). An electroluminescence test was an expedient and safe manner of visually assessing the health of a cell.

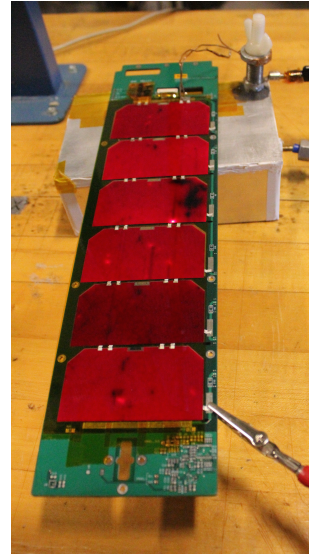


Figure 5: A panel undergoing EL testing.

In this test, a voltage was supplied to the cells in a forward bias configuration that caused electroluminescence. Dark regions were indicative of damage to cell diodes while changing illumination alerted fabricators to cell degradation over the course of the integration process. Importantly, EL testing was a straightforward method of assessing whether a cell shorted; namely, a cell that shorted would not electroluminescence.

Illumination Testing: Each cell was subjected to illumination testing throughout the integration process (post-tabling, post-stringing and post-integration onto PCB). Illumination testing was an effective method of assessing cell performance in on-orbit luminosity conditions. An ARRI Daylight Compact 2500 light was used to produce the desired luminosity conditions. When a cell, a transducer, was exposed to the light source, it generated a current that was used to produce a current-voltage curve (IV-curve). This curve allowed max power of the cell to be calculated and alerted fabricators to degradation in cell performance.

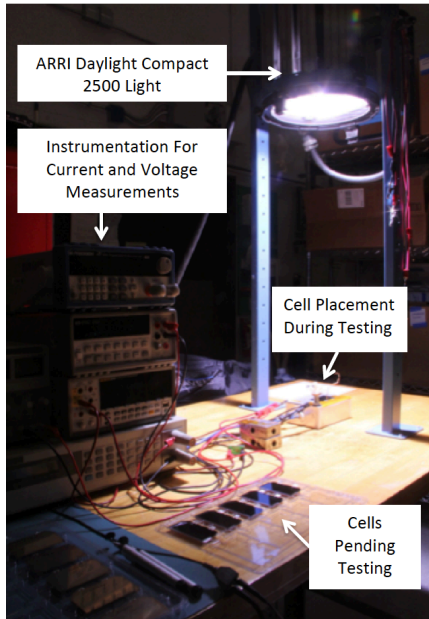


Figure 6: Illumination test set-up.

Infrared (IR) Testing: IR testing was conducted on integrated panels and allowed voids during cell adhesion to be visually observed. IR testing involved exposing a panel to a brief heat source (a flash from a monolight) and using an IR camera to record the behavior of heat dissipation (see Figure 7).

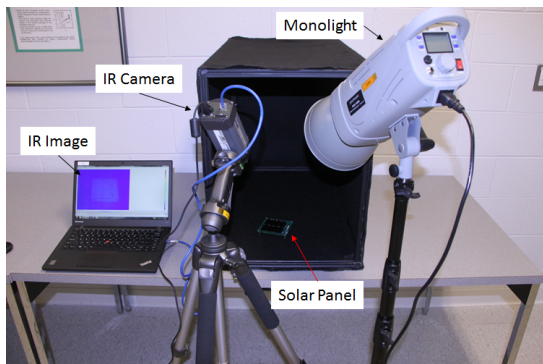


Figure 7: Infrared test set-up.

Regions with voiding were identified by observing that areas with trapped air pockets dissipate heat more slowly than those without voiding (see Figure 8).

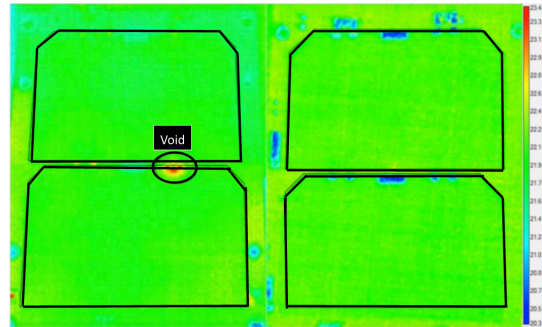


Figure 8: IR image of panel exhibiting voiding.

Preliminary Vacuum Testing: This testing was conducted on integrated panels that did not visually demonstrate voiding under IR testing. This test involved placing the panel in a weak vacuum (~1 torr) produced by an available student test chamber. This vacuum testing exposed any major voids that were overlooked during IR testing (the vacuum is strong enough to cause voided cells to warp). If a cell was observed to have voids, it was de-integrated and replaced.

Vibration Testing: Panels that survived the integration process without degradation (as tracked by EL and illumination testing) or voiding (as tracked by the IR and preliminary vacuum testing) were subjected to vibration testing at University of Michigan’s Space Physics Research Laboratory. The vibration testing had two purposes: 1) to assess panel survival in launch vibration conditions and 2) to assess the resonant frequencies of the panel via sine sweep. Changes in resonant frequency of the panel during testing could indicate panel damage.

Thermal Vacuum Testing: Panels that survived vibration testing were subjected to rigorous thermal-vacuum testing at the Space Physics Research Laboratory. After thermal-vacuum testing, the panels were recharacterized via EL and illumination testing to identify changes in cell performance.

RESULTS

Component Level

The individual procedural changes were tested and compared to heritage methods. Below are the results.

Tabbing: The simplified tabbing procedure decreased tabbing time, increased tabbing yield and decreased risk of cell damage (see Figure 9):

- Tabbing time was reduced by approximately 70% from ~10 minutes to ~3 minutes per cell. Labor was reduced from two fabricators to one.
- The reduction of three heating cycles to one decreased the risk of accidental solder flow and cell shorting, increasing the yield of usable cells per tabbing batch. Using this new method, the shorting rate was reduced from 10% to roughly 3% (3 out of 92 cells shorted compared to 1 out of 10, as verified by EL testing).
- The proposed procedure eliminated the need for weights to increase the robustness of solder joints. Thus, the physical risk of cell fracturing was reduced.

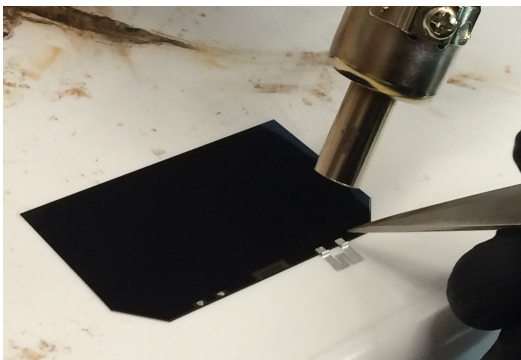


Figure 9: Optimized tabbing procedure employing a reflow gun.

Stringing: Decoupling the cells decreased the risk of cell damage, increased the ease of cell de-integration and allowed versatile orientation of the cells on the PCB:

- Because cells were soldered directly to the substrate and not each other, the integration step requiring weight placement on cell faces was completely eliminated.
- Damaged cells could be successfully de-integrated from panels without impacting other cells in the string. Consequently, strings of cells with damaged cells could be repaired in a timely manner without rendering the entire integrated panel unusable.
- This decoupled cell design does not restrict the orientation of cell placement, allowing that sufficient spacing is placed between cells to allow for soldering of the interconnects to the PCB. For future MXL missions such as TBEx that have complex structural requirements, such versatility of cell placement will be essential (see Figure 11).

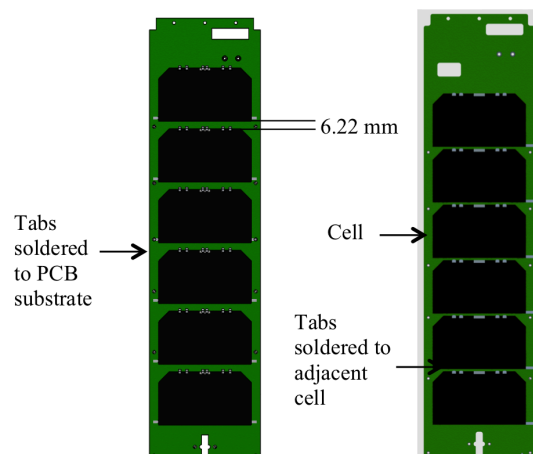


Figure 10: Side-by-side comparison of decoupled panel (left) and coupled CADRE panel (right).

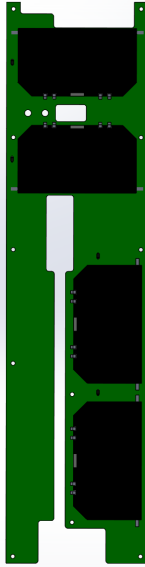


Figure 11: Decoupled panels allow for versatile cell placement, as demonstrated by the TBEx panel above.

Adhering Cells to the PCB: This method demonstrated numerous benefits, including decreasing the incidence of cell voiding, decreasing required integration and curing time, decreasing costs, and allowing damaged cells to be de-integrated from panels:

- As demonstrated by infrared testing, the double-sided Kapton tape visually exhibited less voiding than the silicon adhesive (see Figure 12). The key to such voiding minimization was “vacuum-bagging” the integrated Kapton panel, a process that involved applying homogenous pressure across the cells. Despite the utility of this step in increasing the adhesiveness of the pressure sensitive tape, it induced slight cell warping around the cell side tabs. Though this warping did not cause cell fracturing during preliminary vacuum or thermal-vacuum testing, it warrants further investigation (see Future Work).

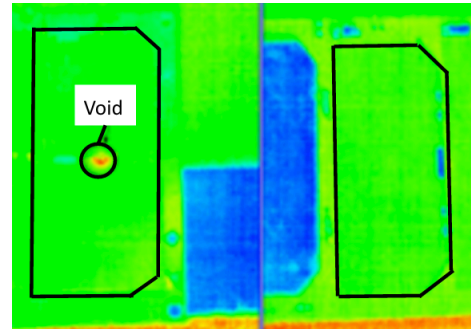


Figure 12: Infrared imaging comparison of cell adhesion with epoxy (left) and Kapton tape (right).

- It reduced the time necessary to integrate and cure a panel. For a panel of six cells, the integration time was reduced from 30-45 minutes to 20 minutes, while the curing time was reduced from four hours to none. When the Kapton tape was pre-cut into the proper shape via laser cutter, the integration time was reduced by an additional 10 minutes.
- It decreased the costs associated with adhering the cells; double-sided Kapton tape is an order of magnitude cheaper than the space-grade silicon adhesive.
- Damaged cells could be easily and efficiently de-integrated from panels. The double-sided Kapton tape, combined with the aforementioned decoupled PCB, allowed individual cells to be de-integrated without harming surrounding cells. In practice, de-integrating a damaged cell from an integrated Kapton panel with this procedure took approximately 30 minutes. This ability to remove and replace cells on integrated panels greatly increased the flexibility and speed of panel manufacturing and repair.

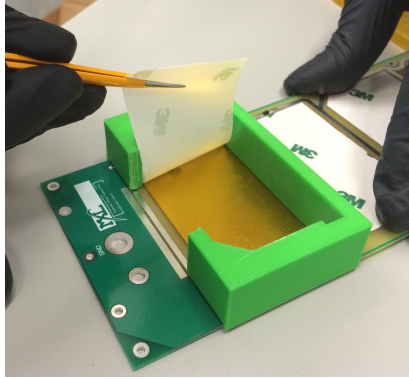


Figure 13: Using Kapton-tape and alignment jig to adhere cells to PCB.

Coverglass: The proposed method of coverglass application was rapid and resulted in minimal loss of power (see Figure 14):

- After an initial mixing time of two minutes, the coverglass epoxy required approximately 15 minutes per dozen cells to apply. Curing at 65C was required for one hour.
- Illumination testing on a sample of 30 cells indicated that cells integrated with coverglass experienced a power loss of less than 2%. This loss in power is likely attributable to the adhesive not being perfectly optically clear.

It is important to note that the coverglass epoxy discussed in this paper, which has a silicon-base, may not be suitable for missions with sensitive scientific instruments (silicon is famously difficult to clean off optics). Though testing alternatives lies outside the scope of this paper, Azur Space endorses Dow Corning 93-500 Space Grade encapsulate as an industry standard for coverglass adhesion, as communicated electronically by their Sales Assistant Michael Preissner.

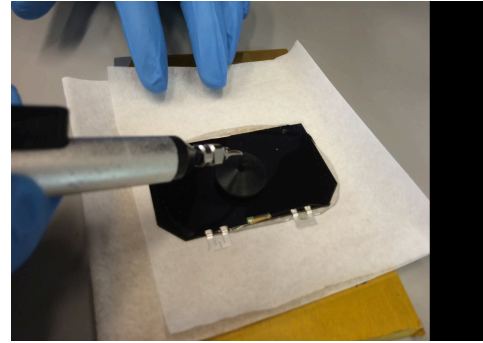


Figure 14: Applying coverglass to bare cell.

Integrated System Level

After determination of the benefits of the procedural changes as distinct integration steps, the procedural adjustments were tested as a complete system; namely, they underwent vibration and thermal-vacuum testing.

Vibration Testing: A culminating verification test of the assembled solar subsystem is vibration testing. For this test, two panels of six cells were prepared: one with cells assembled with coverglass, one without. Both panels, which used decoupled PCBs, utilized the Kapton tape method for cell adhesion. The panels were mounted on a test CubeSat bus (ShakeSat) that was fastened within a 3U CalPoly Test-POD. The panels were subjected to sine sweeps and random vibration profiles at 11 and 22.5 Grms.. Over the course of the testing, no structural failures occurred that resulted in debris. However, damage was incurred on two cells due to set-up and a yet unidentified cause.

During testing, accelerometers were attached to the panels in order to measure frequency responses of the boards. During the 22.5G testing, the accelerometer detached from the panel composed of cells with coverglass, impacting the top cell. This impact resulted in cell damage, as seen during EL testing (see Figure 15).

Fortunately, the protective qualities of the coverglass appeared to decrease the debris that was produced by this impact. No other cells in the string experienced damage. Thus, the damage incurred by this cell is attributable to a failure in the testing set-up, not a failure in the procedural changes.

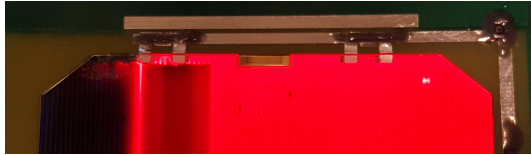


Figure 15: EL testing reveals damage to one cell with coverglass. Damage attributable to set-up failure.

Limited damage was also observed on the non-coverglass panel. The cell nearest to the accelerometer exhibited fractures near the ‘M’ interconnects. Damage was evident during EL testing (see Figure 16). Several hypotheses currently exist as to the cause of this fracturing, including mishandling of the cell prior to vibrate testing and voiding of the cell in the region of the tabs. Future experiments will need to be conducted to link the incident to a definite cause (see Future Work).

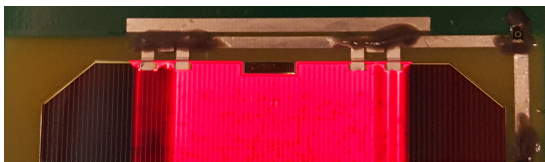


Figure 16: EL testing reveals damage to one cell without coverglass. Cause unknown.

The frequency results of the vibration testing produced by SPRL may also reflect damage to the cells. After the 11G test, the panels experienced a slight change in stiffness along the z and y-axis (see Table 1). This change in stiffness could be indicative of a component of the ShakeSat, independent of the solar panels, coming loose; it could also be indicative of the

decrease in panel stiffness expected after cells fracture.

Table 1: Natural frequencies of the panel under 3-axis vibration.

Vibration Axis	Frequency (Hz)		
	Base	Post-11g	Post-22g
x-axis	416.6	424.3	432.2
y-axis	393.3	378.2	362.8
z-axis	438.2	388.8	374.7

During testing, damage was observed on the above discussed cells following the 22.5G test, not the 11G test. Thus, the decline in resonant frequency after the 11G test is perhaps more likely attributable to a structural shift in the ShakeSat itself. Future investigations into solar cell voiding will hopefully shed light on this issue (see Future Work).

The damage incurred by the two cells manifested in the results of illumination testing conducted post-vibration testing. As can be seen from the graph below, both the coverglass and non-coverglass panel lost approximately 1W of power output post-vibration testing (see Figure 17). The nominal value comes from the assumption that a string of six cells will produce 6W of power when fully functioning (1W per cell).

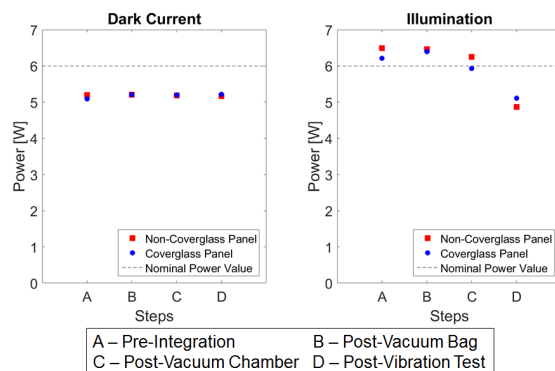


Figure 17: Power output decreased by 1W post-vibe for both panels.

This loss in power is characteristic of one cell in each string failing to produce power; indeed, upon further testing, it was determined that the damaged cells in both strings were causing their bypass diodes to kick-in, preventing these cells from contributing 1W of power to the panel. This conclusion was drawn from analyzing the IV-curves generated via illumination testing prior to and post-vibration testing (see Figure 18).

The observed step-function like feature of the post-vibe IV-curve is characteristic of the activation of one the cell's bypass diodes, as can be seen in Figure 19. Though Figure 18 corresponds to the panel with coverglass, the same behavior was observed under illumination testing for the panel without coverglass.

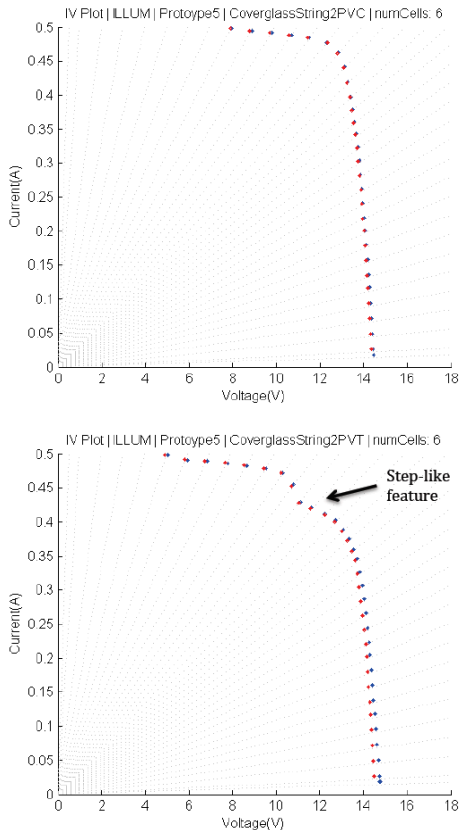


Figure 18: IV-curve of panel with coverglass prior to vibration testing (top) and post-vibration testing (bottom).

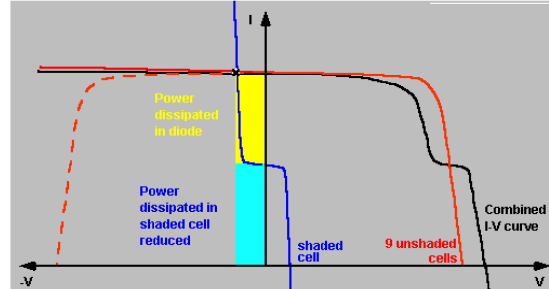


Figure 19: Graph depicting effects of bypass diodes on IV-curve. Credit: Baghzouz⁽¹⁾

Thermal-Vacuum Testing: The same two panels that were subjected to vibration testing underwent thermal-vacuum testing; however, the two fractured cells were successfully de-integrated and replaced. The panels underwent eight thermal cycles of -45C to +60C at $\sim 1 \cdot 10^{-6}$ torr. Illumination testing following the thermal-vacuum testing indicated that the panels lost approximately 0.01W of power, which was deemed negligible in the scope of the mission's general power budget.

FUTURE WORK

In light of available test results and the observed benefits of the procedural changes, MXL will be incorporating the new procedure into its upcoming TBEx flight build. However, further investigation is warranted in certain areas; namely, the observed warping around the cell's side tab post-vacuum bagging and the unaccounted for cell fracturing during vibration testing.

The observed cell warping may be due to localized stacking of the side tab on the Kapton tape. The cell's side tab has a maximum height of 0.00178" (see Figure 20). For the investigation presented in this paper, no Kapton was cut away beneath this tab; thus, the part of the cell with the side tab was 0.00178" higher than the rest of the cell. This height offset could allow a non-negligible air pocket beneath the cell to

form, resulting in cell damage. It is suspected that cutting out the Kapton beneath the side tab will diminish the impact of this height offset, decreasing the stress placed on the cell in this region and the observed voiding. A test panel will be produced to test this hypothesis.

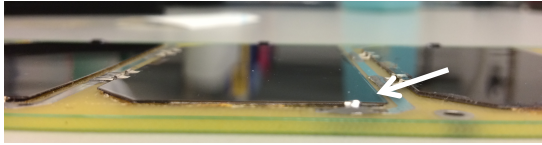


Figure 20: Kapton-side tab interface. Side tab raises cell 0.00178” higher than rest of cell.

Additionally, an investigation will be conducted into the cause of the cell fracturing during vibration testing. An engineering design model of the solar subsystem will be produced for the TBEx mission implementing these design changes. This subsystem will be subjected to similar vibration testing conditions; it is hoped that the reproducibility or non-reproducibility of the damage will shed light on the cause.

CONCLUSION

The streamlined solar panel fabrication process greatly increases the yield, cost effectiveness and reliability of the solar panel subsystem. It enables a solar panel to be fabricated from tabbing to coverglass application in a single day without compromising quality or flight performance, adding crucial flexibility to tight flight build schedules. In a larger sense, this process, through its improvements to solar panel reliability and manufacturability, contributes to the knowledge base that allows small satellites to be used as meaningful tools of science. Since demonstrating its robustness via rigorous verification testing, this procedure

will be implemented on MXL’s upcoming TBEx CubeSat mission.

Acknowledgements

It takes a village. I wish to thank Dr. Smith, Dr. James Cutler and Tyler Rose for their continued guidance and insight throughout this investigation. I would like to thank Emanuela Della Bosca, Brian Shaw, Gregorio Lopez, and Andrew Plave for their support in executing the experiments. Lastly, I would like to extend my deepest gratitude to Andrew Dahir and James Mason of the Colorado small satellite community for their willingness to collaborate and share their personal experience.

References

1. Baghzouz, Y. "Photovoltaic Devices III." (n.d.): n. pag. *EE 446/646*. University of Nevada, Las Vegas. Web. 18 Dec. 2015.
2. Dahir, Andrew. "Edited Solar Cell Mounting Procedure." University of Colorado-Boulder, 2015. Web. 20 Dec. 2015.
3. Danzilio, David. "Overview of EMCORE’s Multi-junction Solar Cell Technology and High Volume Manufacturing Capabilities." (n.d.): n. pag. *Csmantech.org*. CS MANTECH Conference, 14 May 2007. Web. 14 Dec. 2015.
4. Karuza, Petras, and David A. Hinkley. "Solar Cell Installation Using Double Sided Polysiloxane Pressure Sensitive Adhesive (PSA) Polyimide Film." *Cal Poly*. The Aerospace Corporation, 2009. Web. 23 Dec. 2015.
5. Mason, James, and Bena Mero. "MinXSS Solar Cell Mounting FAI." Laboratory for Atmospheric and

Space Physics, 2015. Web. 20 Dec. 2015.

6. Schaffner, Jake A. "The Electronic System Design, Analysis, Integration, and Construction of the Cal Poly State University CP1 CubeSat." *Digital Commons - Utah State University*. AIAA/USU Conference on Small Satellites, 2002. Web. 20 Dec. 2015.
7. Shaffer, Chris, Ryan Caron, and Vassilis Angelopoulos. "Study of the Need for Solar Panel Coverglass for CubeSat Missions." (n.d.): n. pag. *Electron Losses and Fields Investigation (ELFIN)*. Department of Earth and Space Sciences: Institute of Geophysics and Planetary Physics, UCLA. Web. 18 Dec. 2015.